THE JOURNAL OF BIOLOGICAL CHEMISTRY VOL. 287, NO. 11, pp. 8507–8514, March 9, 2012
Published in the U.S.A.

High Throughput Engineering to Revitalize a Vestigial Electron Transfer Pathway in Bacterial Photosynthetic Reaction Centers*[S]

Received for publication, November 22, 2011, and in revised form, January 6, 2012 Published, JBC Papers in Press, January 14, 2012, DOI 10.1074/jbc.M111.326447

Kaitlyn M. Faries[‡1], Lucas L. Kressel[§1], Marc J. Wander[§1], Dewey Holten[‡], Philip D. Laible[§], Christine Kirmaier[‡2], and Deborah K. Hanson[§3]

From the [‡]Department of Chemistry, Washington University, St. Louis, Missouri 63130 and the [§]Biosciences Division, Argonne National Laboratory, Argonne, Illinois 60439

Background: Bacterial reaction centers catalyze light-induced transmembrane electron transport using only one of two chemically equivalent pathways.
Results: Multiplexed screening uncovers semirandom mutations that unexpectedly activate the unused pathway by employing ionizable residues.
Conclusion: High throughput mutagenesis approaches reveal structure/function relationships that govern electron transfer efficiency.
Significance: Directed molecular evolution can reveal principles that enable efficient, unidirectional, transmembrane electron transfer for the design of *de novo* pathways or biomimetic devices.

Photosynthetic reaction centers convert light energy into chemical energy in a series of transmembrane electron transfer reactions, each with near 100% yield. The structures of reaction centers reveal two symmetry-related branches of cofactors (denoted A and B) that are functionally asymmetric; purple bacterial reaction centers use the A pathway exclusively. Previously, site-specific mutagenesis has yielded reaction centers capable of transmembrane charge separation solely via the B branch cofactors, but the best overall electron transfer yields are still low. In an attempt to better realize the architectural and energetic factors that underlie the directionality and yields of electron transfer, sites within the protein-cofactor complex were targeted in a directed molecular evolution strategy that implements streamlined mutagenesis and high throughput spectroscopic screening. The polycistronic approach enables efficient construction and expression of a large number of variants of a heteroligomeric complex that has two intimately regulated subunits with high sequence similarity, common features of many prokaryotic and eukaryotic transmembrane protein assemblies. The strategy has succeeded in the discovery of several mutant reaction centers with increased efficiency of the B pathway; they carry multiple substitutions that have not been explored or linked using traditional approaches. This work expands our understanding of the structure-function relationships that dictate the efficiency of biological energy-conversion reactions, concepts that will aid the design of bio-inspired assemblies capable of both efficient charge separation and charge stabilization.

Light energy is converted to chemical energy in a series of extremely efficient electron transfer (ET)[4] reactions performed by photosynthetic reaction centers (RCs). The structures of these transmembrane protein-cofactor complexes from photosynthetic bacteria and higher plants reveal an axis of approximate 2-fold symmetry that relates both core protein subunits and functionally asymmetric sets of cofactors (Fig. 1) (1–4). In many photosynthetic bacteria, these complexes are composed of three subunits: the homologous, integral L and M polypeptides and the membrane-tethered H polypeptide. Bacterial cofactors include a bacteriochlorophyll dimer (P) that serves as the primary electron donor, two bacteriochlorophyll monomers (B_A and B_B), two bacteriopheophytins (H_A and H_B), and two ubiquinone$_{10}$ molecules (Q_A and Q_B). In type I RCs (*e.g.* Photosystem I), spectroscopic evidence suggests that both pathways are active in producing reduced quinone via light-induced ET (see *e.g.* Refs. 5–8). Yet, in type II RCs (*e.g.* bacterial RCs and Photosystem II), the B pathway is silent, and possibly vestigial; only the A branch cofactors are active.

The relative free energies of the charge-separated states are critical in determining the directionality, rates, and yields of ET in the RC. Some strategies to manipulate these factors genetically over the last 20 years (for review, see Ref. 9) include: addition or removal of hydrogen bonds to cofactors (10–15); addi-

* This work was supported by Grant DE-FG-02-09ER16116 from the United States Department of Energy Office of Basic Energy Sciences, Division of Chemical Sciences, Geosciences, and Biosciences (to C. K., D. H., P. D. L., and D. K. H.). Argonne, a United States Department of Energy Office of Science laboratory, is operated under Contract DE-AC02-06CH11357.
[S] This article contains supplemental Tables S1–S4 and Methods.
The nucleotide sequence(s) reported in this paper has been submitted to the GenBank™/EBI Data Bank with accession number(s) JN565028.
[1] These authors contributed equally to this work.
[2] To whom correspondence may be addressed. Tel.: 314-935-6480; Fax: 314-935-4481; E-mail: kirmaier@wustl.edu.
[3] To whom correspondence may be addressed. Tel.: 630-252-4189; Fax: 630-252-3387; E-mail: dkhanson@anl.gov.

[4] The abbreviations used are: ET, electron transfer; B, bacteriochlorophyll; H, bacteriopheophytin; LH, light harvesting; Q, quinone; P, primary donor; RC, reaction center; YFHV, F(L181)Y-Y(M208)F-L(M212)H-W(M250)V; KFHV, F(L181)K+FHV; AA+YFHV, E(L212)A-D(L213)A+YFHV; HFHV, F(L181)H+FHV; NFHV, F(L181)N+FHV; DFHV, F(L181)D+FHV; WFHV, F(181)W+FHV.

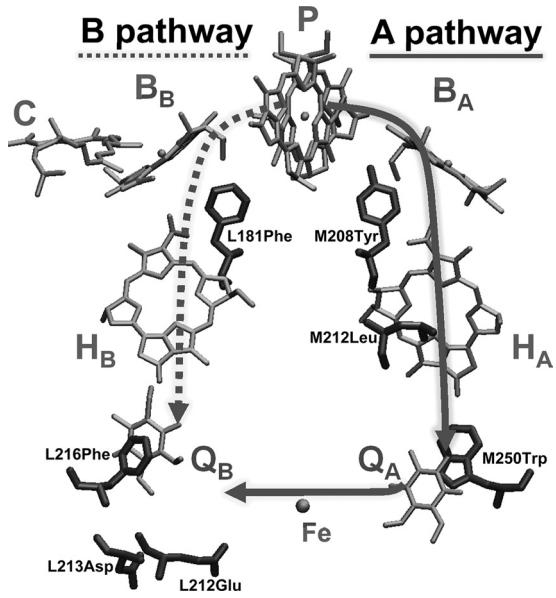

FIGURE 1. **Electron transfer pathways and positions of substituted amino acids in bacterial RCs.** Despite equivalent sets of symmetry-related cofactors, only the A branch is active in native RCs. For visual clarity, all isoprenyl anchoring groups and bulky porphyrin ring substituents were removed from cofactors.

tion or removal of axial ligands with attendant changes of bacteriopheophytin to bacteriochlorophyll or vice versa (16–27); modification of conserved residues or helical segments that are related by the pseudo-2-fold symmetry axis of the complex (28, 29); and introduction or removal of polar or ionizable residues near the cofactors (12, 13, 16, 17, 30–32). To disable ET from H_A to Q_A or from Q_A to Q_B specifically, the occupancy and environments of the quinone binding pockets have been manipulated by mutation (16, 23–25, 33–37).

The highest yields of ET from the excited dimer (P*) to H_B (thus producing $P^+H_B^-$) have been achieved in mutant *Rhodobacter* (*R.*) *capsulatus* RCs (17, 31, 32, 35, 38). In mutant RCs lacking Q_A, reduction of Q_B via sole activity of the B branch cofactors has been observed unambiguously (16, 24, 35, 37, 39–41). No cases yet reproduce any of the (essentially) 100% yields characteristic of the native A side ET reactions. Rather, mutant RCs have demonstrated the magnitude of the B pathway inefficiency. The combination of a few site-specific mutations has not managed to modulate the energetics (or electronic factors) of the B branch cofactors to provide for rapid electron transfer. At present, we lack the understanding needed to use rational design to accomplish the drastic leap required to redesign the RC to use the B pathway exclusively and efficiently.

Construction of such a re-engineered RC requires sampling of a much larger number of variants than has been examined previously. Thus, an approach has been adopted that combines semirandom mutagenesis and rapid screening techniques that require minimal sample volumes. Several methods have been streamlined by implementation of an automated liquid handler, and purification of mutant RCs has been semiautomated. A high throughput spectroscopic assay evaluates the competency of candidate RCs for Q_B reduction via the B side cofactors. This approach has been made feasible by advances in synthetic biology; favorable mutations that have been identified can be fed into directed molecular evolution experiments for additional optimization of the ET pathway. Techniques that have been developed here are likely to be applicable to other multisubunit protein complexes with similar gene architectures.

EXPERIMENTAL PROCEDURES

Growth—R. capsulatus strains were cultured on ^{Super}RCVPY (20) medium under semiaerobic, chemoheterotrophic conditions in the dark (165 rpm, silicone sponge closures, 33 °C). *Escherichia coli* strains were propagated on LB or 2×TY medium (42). Plasmids were selected with kanamycin (30 μg/ml for both organisms). Strains and plasmids used in this study are listed in supplemental Table S1.

Molecular Biology—The expression vector used in this study, pBBRKW2HTsLsM (Fig. 2; GenBank Accession Number JN565028), was constructed from *puf* operon genes derived as an EcoRI-SacI fragment from plasmid pUHTMluBgl:α^- (24) that was inserted into a derivative of broad host range cloning vector pBBR1MCS-2 (43), generating pBBRKW2HTBALMX. The expression plasmid was then modified extensively to facilitate the approach described herein. Portions of both the *puf*L and *puf*M genes were synthesized (GenScript) to encode silent changes that introduced restriction sites flanking each of the segments chosen for mutagenesis (Fig. 2). To eliminate duplicate restriction sites elsewhere, 11 restriction sites in pBBR1MCS-2 and 4 sites in the *puf* operon were removed (supplemental Table S2) using either site-directed mutagenesis (QuikChange; Stratagene) or mung bean nuclease. The synthetic segment of *puf*L was then cloned into pBBRKW2HTBALM*X* (Table S2) as a PstI-KpnI fragment, and the synthetic *puf*M segment was cloned using BglII and BamHI, thus creating pBBRKW2HTsLsM. A His_7 tag is encoded at the C terminus of *puf*M. The H32R mutation in the *puf*A gene prevents assembly of the light-harvesting (LH) I antenna complex (44). Thus, genes expressed from this plasmid in *R. capsulatus* strain U43 result in the antennaeless, "RC-only" photosynthetic membrane needed for quantitative extraction of RCs by mild detergents (24). A summary of substitutions carried by mutant RCs and the nomenclature used to refer to them is contained in supplemental Table S3.

Construction of the F(L181)*X*+FHV, F(L216)*X*+YFHV and E(L212)A-D(L213)A-F(L216)*X*+YFHV sets of mutant strains was expedited with cassette-based mutagenesis. The W(M250)V control strain was constructed by site-directed mutagenesis of the synthetic BglII-BamHI fragment of the *puf*M segment described above. Protocols for phosphorylation and annealing of oligonucleotides, ligations, transformations, and plasmid screening were adapted for use with a liquid handling system (Biomek FX; Beckman Coulter). For each mutant set, a library of oligonucleotides was designed to encode all 20 amino acids at residue *X*. Oligonucleotides for the F(L181)*X*+FHV set were flanked by HindIII and BbvCI restriction sites, and the oligonucleotides for the F(L216)*X*+YFHV and E(L212)A-D(L213)A-F(L216)*X*+YFHV cassettes were flanked by AccIII and AclI restriction sites (Table 1 and Fig. 2). Oligonucleotides were phosphorylated, annealed, and ligated to pBBRKW2HTsLsM digested with the appropriate restriction enzymes. Candidate plasmids from DH5α transformants

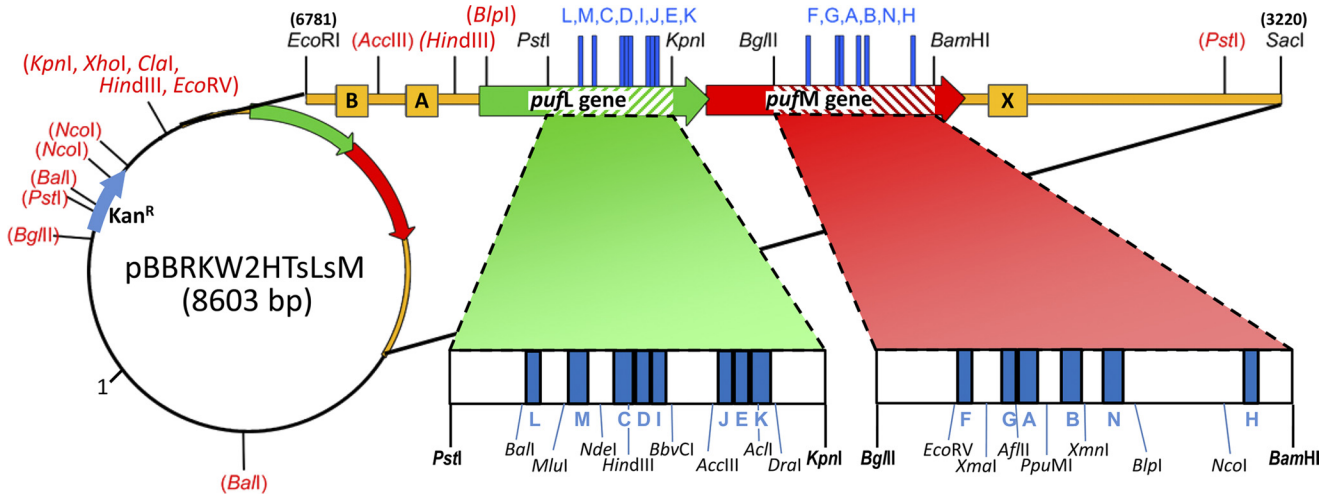

FIGURE 2. **Engineered expression plasmid for RC mutagenesis.** Segments of the L and M genes targeted for mutagenesis (*striped regions* and Table 1) are flanked by unique restriction sites that facilitate the insertions of oligonucleotide cassettes encoding multiple substitutions. Fifteen restriction sites (*parentheses*) in the plasmid were removed to enable the cassette-based mutagenesis approach.

TABLE 1
Regions targeted for mutagenesis

Cofactor	Amino acid segment (region)	5′-Flanking enzyme	3′-Flanking enzyme
B_B	M150–160 (A)	AflII	PpuMI
B_B	M173–184 (B)	PpuMI	XmnI
B_B	L168–178 (C)	NdeI	HindIII
B_B/H_B	L179–190 (D)	HindIII	BbvCI
H_B	L215–220 (E)	AccIII	AclI
H_B	M124–131 (F)	EcoRV	XmaI
H_B	M144–151 (G)	XmaI	AflII
H_B	M271–275 (H)	NcoI	BamHI
Q_B	L186–194 (I)	HindIII	BbvCI
Q_B	L212- 216 (J)	AccIII	AclI
Q_B	L220–232 (K)	AclI	DraI
B_A	L127–131 (L)	BalI	MluI
B_A	L146–157 (M)	MluI	NdeI
B_A	M195–207 (N)	XmnI	BlpI

were screened using restriction fragment analysis and sequenced. Correct plasmids were used to transform mobilizing donor strain S17-1 for conjugal transfer to *R. capsulatus* deletion strain U43 (24). To facilitate rapid recovery of expression strains, a 100-μl aliquot of a 1:25,000 dilution in RCV medium (45) was plated directly to ^{Super}RCVPY agar containing kanamycin. After 2 days, *R. capsulatus* colonies were cultured on ^{Super}RCVPY containing kanamycin for the preparation of archival stocks.

Expression Screening—To survey expression levels, crude RCs were purified in tandem according to standard methods (as detailed in supplemental Methods) with the following modifications. Cells from small cultures (80 ml) were lysed using a microfluidizer (Microfluidics, Inc.) and mutant RCs were solubilized with Deriphat 160-C. Following overnight binding to 200 μl of nickel-nitrilotriacetic acid resin (Qiagen), chromatography proceeded in 2-ml, 96-well filter plates. UV-visible spectra of dark-adapted (10 min) samples were recorded (SpectraMax M5^e; Molecular Devices). Based on $A_{865\ nm}$, mutant RCs were classified into three expression categories relative to yields of WT RCs: abundant (>25%), moderate (2.5–25%), and poor (<2.5%).

Semiautomated RC Purification—Mutant strains that expressed RCs abundantly or moderately were grown in 2–6-liter volumes depending on the expression level. RCs were purified via semiautomated methods using ÄKTA-FPLCs (46).

RC Functionality Screening—Assaying mutant RCs for formation of $P^+Q_B^-$ via B branch ET was accomplished with a home-built, time-resolved spectrometer designed for 100–200-μl samples arrayed in clear-bottom 96-well plates (BD Falcon). Rapid data collection and reproducibility were facilitated via use of a computer-controlled translation stage (Aerotech) to position the sample well under collinear, vertical excitation and probing (measuring) beams. RCs were excited with a single subsaturating, 5-ns, 532-nm flash from a Nd:YAG laser. The magnitude and decay of bleaching of the ground state absorbance of P were probed by a stable, continuous-wave, 850-nm laser diode (Melles-Griot) attenuated with neutral density filters so that no discernible actinic effects were observed. For added sample protection, the probe light was incident on the sample only during data collection and was otherwise blocked with a computer-controlled shutter. Following passage through the sample, the probe light was isolated from the collinearized pump-probe beams by dichroic and 850-nm interference filters. The isolated probe light was collected onto a near-infrared-sensitive photosensor module (Hamamatsu H-5784-20), whose output was recorded on a digital oscilloscope. The apparatus is capable of measuring transient spectroscopic signals

spanning 50 μs to several minutes. For 100-μl volume, the effective measuring pathlength was 2 mm; sample concentrations were adjusted such that $A_{865\,nm}$ was 0.45–0.55. Signal intensities were normalized to the same ground state absorbance of the P band during data analysis. Because RCs are Q_A-less (except for wild type) due to the W(M250)V mutation described below, the initial amplitude of each kinetic trace is proportional to the yield of ET to Q_B solely via the B branch, as assayed relative to control RCs on the same plate.

Further characterization of primary electron transfer events in select mutant RCs utilized a transient absorption apparatus having 130-fs excitation and white light probe flashes operating at 10 Hz (described previously in Refs. 31, 38). RCs were held at ~10 °C in an ice-cooled reservoir and flowed through a 2-mm pathlength cell.

RESULTS

A system to construct and express mutants of the L and M genes of the polycistronic, oxygen-regulated *puf* operon of *R. capsulatus* was developed previously (47–49). The expression host strain, U43, does not synthesize any light-harvesting antennae or RC complexes of the photosynthetic apparatus (*i.e.* LHI^- $LHII^-$ RC^-). The original broad host range expression plasmid cannot be used for this type of study because its complete sequence has not been determined and its large size (32 kb) hinders its application to an approach based upon restriction enzyme cloning of mutated cassettes. Thus, pBBR1MCS-2 (5.1 kb), whose sequence is known (43), was selected as the vector for the expression plasmid and modified as described above. Yields of RCs purified from strains carrying the newly engineered expression plasmid were found to be 2-fold greater than those obtained from plasmid pUHTMluBgl:α^-.

The initial mutagenesis template was FHV. The F mutation substitutes Phe for the native Tyr at M208 near B_A and diminishes ET to the A side. The H mutation substitutes His for Leu at M212 near H_A and results in incorporation of a bacteriochlorophyll in the H_A site. Because this cofactor is more difficult to reduce, the A pathway is disabled further. This mutation also removes H_A absorption from the 510–550 nm spectral region, allowing quantitative assessment of H_B reduction via ultrafast (picosecond) spectroscopic measurements. The V mutation, which substitutes Val for the conserved Trp at M250, prevents Q_A binding and, thus, prevents ET to Q_B via Q_A. In other words, this mutation ensures that electrons can reach Q_B only via the B side cofactors.

M208Tyr is related via the C_2 symmetry axis to residue L181Phe near B_B. This conserved asymmetric pair was the target of some of the earliest mutagenesis studies of the purple bacterial RC. The swap of Tyr for the native Phe at L181 and Phe for Tyr at M208 reverses the asymmetry and enhances ET to H_B while diminishing ET to the A side. When the F(L181)Y mutation is added to the FHV template, the result is the YFHV RC, which serves as another control (in addition to the wild type that results in quantitative reduction of Q_B via A branch activity) for the ms screening assay because it displays ~30% yield of $P^+H_B^-$ and ~15% yield of $P^+Q_B^-$ (31, 35, 39, 40, 50).

A large number of residues within 5–14 amino acid segments near the cofactors have been identified as mutagenesis targets

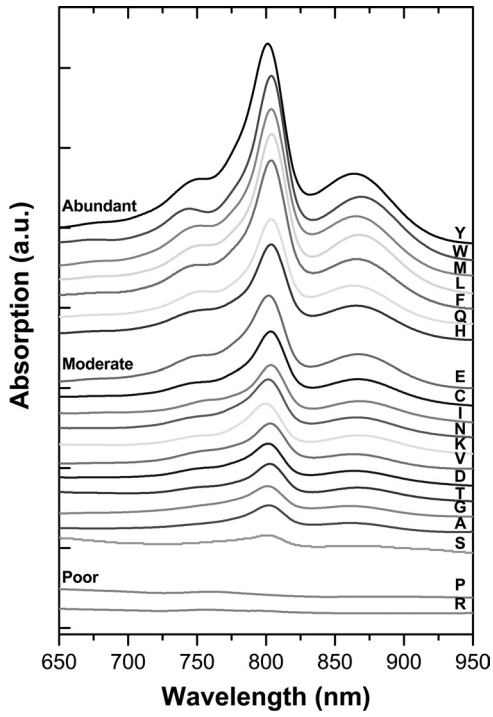

FIGURE 3. **Expression yields of mutant RCs.** UV-visible spectra of RCs purified from the F(L181)*X*+FHV set of mutant RCs indicate three expression categories. The residue present at the L181 site is designated with the single-letter code.

(Table 1 and Fig. 2). At the outset, regions proximal to B_B, H_B, and Q_B were targeted to further enable (compared with YFHV) the B side pathway. For all of the mutant strains reported here, protein yields from larger scale cultures and automated purification procedures correlated well with yields determined from the small scale expression screening. The use of Deriphat 160C for RC solubilization and purification ensured full occupancy of Q_B in the native binding site (24).

Twenty F(L181)*X*+FHV constructs comprised the initial mutant set. Residue L181 (segment D, near B_B) was chosen because of the known influence of this site on initial B side charge separation as indicated above. Eighteen of the mutant RCs were expressed moderately or abundantly (Fig. 3). None of the substitutions at L181 resulted in pronounced effects on the RC ground state absorption spectra except for the KFHV mutant, with K at L181 previously having been shown to provide a sixth ligand to B_B (11).

Additional rounds of mutagenesis focused on residues near Q_B in attempts to increase the low (~40%) yield of ET from H_B to Q_B (24, 35, 39). Saturation mutagenesis was performed at conserved residue L216Phe (segment J) because its C_2-symmetry-related counterpart, M250Trp, is essential for rapid ET from H_A to Q_A (33) and is important for Q_A binding. The F(L216)*X* substitutions were coupled with YFHV. Additionally, because previous work showed that replacement of the native Glu and Asp at L212 and L213, respectively, with alanines stabilizes $P^+Q_B^-$ (51), the F(L216)*X* variants were coupled with the E(L212)A-D(L213)A+YFHV (AA+YFHV) substitutions in another set of mutants. These two rounds of mutagenesis yielded 40 additional strains with 36 expressing RCs at abundant or moderate levels, 19 F(L216)*X*+YFHV mutants and 17

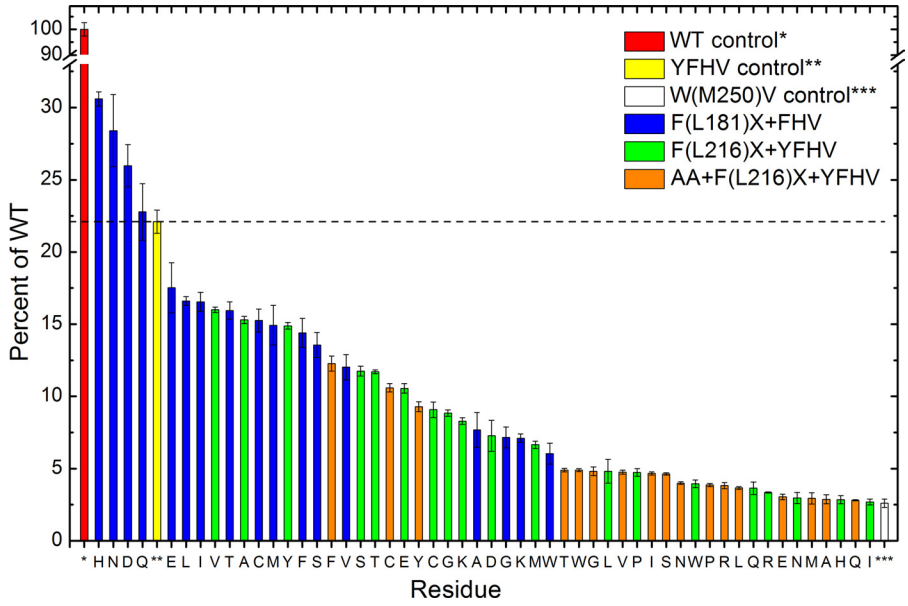

FIGURE 4. **B branch quinone reduction in mutant RCs.** Yields of B side $P^+Q_B^-$ formation from time-resolved assays of mutant RCs relative to signals from wild-type RCs are shown. Signals from the YFHV (*yellow*) and W(M250)V (*white*) RCs serve as benchmark controls. *Error bars* reflect variability in replicate spectroscopic screening measurements.

AA+F(L216)*X*+YFHV mutants (supplemental Table S4). Only the D, H, and K substitutions failed to produce RCs in the AA+F(L216)*X*+YFHV background.

All 54 of the mutant RCs studied here gave light-induced formation of $P^+Q_B^-$ via the B side cofactors in the ms transient absorption assay. The relative amounts of $P^+Q_B^-$ formed are plotted in Fig. 4. Of particular note are the F(L181)H+FHV (HFHV), F(L181)N+FHV (NFHV), and F(L181)D+FHV (DFHV) mutant RCs, which produce $P^+Q_B^-$ signals that are 20–30% larger than that of the YFHV control. The A, G, K, and W mutations produce RCs with the poorest yields of $P^+Q_B^-$ in the F(L181)*X*+FHV series. Fig. 5*A* shows kinetic traces derived from the HFHV, NFHV, DFHV, and WFHV RCs along with the YFHV and W(M250)V-only control RCs from the ms screening assay. The profiles, displaying decay time constants ≥10 s, are characteristic of $P^+Q_B^-$ charge recombination when this state is formed via activity of the B branch cofactors; in these RCs, decay of this state via routes involving Q_A is prohibited by the W(M250)V mutation (24). Thus, the initial amplitudes of the kinetic traces in Fig. 5*A* are measures of the (relative) yields of $P^+Q_B^-$ formed solely via B branch activity; this value is plotted for all of the mutant RCs in Fig. 4.

The results for the HFHV, NFHV, DFHV, and WFHV mutant RCs were confirmed by ultrafast transient absorption measurements (Fig. 5*B*). These spectra show the magnitudes of bleaching of H_B at ~528 nm, reflecting the relative yields of ET from P* to H_B and confirm an ordering of H>N>D>Y≫W, the same ordering as determined in the $P^+Q_B^-$ yield assay. Additional ultrafast measurements are under way and will be reported elsewhere.

Expression yields for the F(L216)*X*+YFHV and AA+F(L216)*X*+YFHV sets of mutant RCs were quite high, especially for the latter set given the number of mutations introduced into the RC. However, yields of $P^+Q_B^-$ in these mutant RCs did not exceed that of the template YFHV. In general, there is less ET to Q_B in RCs containing the E(L212)A-D(L213)A substitutions than in mutant RCs carrying the native residues at these sites. The relative rank order of the residues in each set is different (see, *e.g.* the effect of a Val substitution in each set), suggesting complex interplay of effects introduced by substitution of the small, nonpolar alanines for the larger, ionizable Glu and Asp.

DISCUSSION

Directionality of ET in type II RCs is a conundrum that has existed ever since the 1985 structure of the bacterial RC (3) revealed two branches of cofactors related by an axis of approximate C_2 symmetry whereas spectroscopic measurements demonstrated activity of only one of them. The free energies of the charge-separated states on the A pathway ($P^+B_A^-$, $P^+H_A^-$, and $P^+Q_A^-$) are successively downhill from each other and from P*, facilitating rapid forward ET. In contrast, B branch inactivity presumably stems in large measure from $P^+B_B^-$ being somewhat higher in free energy than P*, resulting in much slower, noncompetitive, B side charge separation. Differences between the electronic couplings of P* with B_A and B_B may also contribute to unidirectional A side ET. The rate constant for $P^* \rightarrow P^+H_B^-$ on the native B pathway has been measured to be ~$(100\ ps)^{-1}$ (17, 31), approximately 30-fold slower than charge separation on the A side (3–4 ps for $P^* \rightarrow P^+H_A^-$), suggesting that yields of B side ET in wild-type RCs should be ~3%.

Although significant yields of $P^+H_B^-$ formation have been reported in some *R. capsulatus* mutants (17, 31, 32, 35, 38), the largest rate constant for $P^* \rightarrow P^+H_B^-$ is ~$(40\ ps)^{-1}$, obtained in the YFH mutant RC (31). The best efforts by several laboratories over many years have thus achieved approximately only a 2-fold increase in the rate of ET to H_B compared with the wild-type value. This enhanced rate is still a factor of 10 slower than ET to the A side. Interestingly, rapid initial charge separation to the B side has been reported in a mutant where a bacteriopheo-

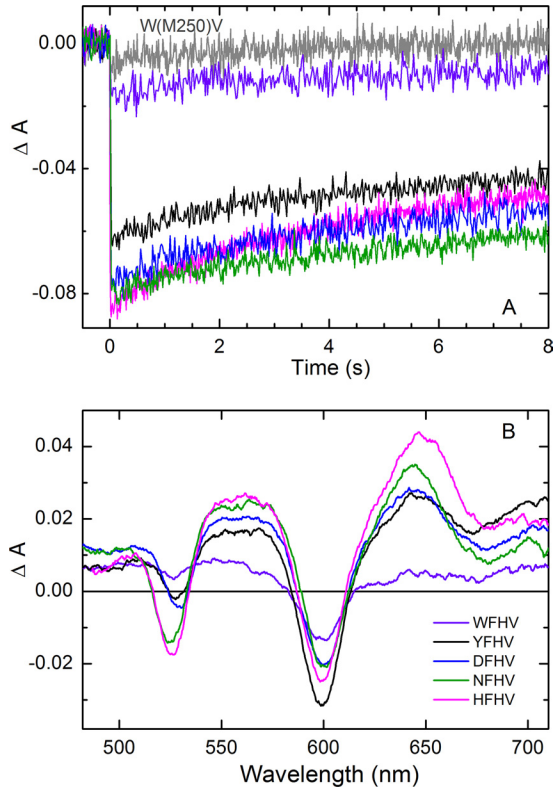

FIGURE 5. **Transient light-induced optical signals indicative of B branch activity in mutant RCs.** *A*, P-bleaching amplitudes and decay profiles for state $P^+Q_B^-$ observed in the ms screening assay. The *gray trace* is for the W(M250)V mutant RC; the other *traces* are as indicated in the legend in *B*. Each *trace* represents the average of seven data acquisitions (single excitation flash events). Signal amplitudes were corrected by factors of ≤1.2 to normalize the sample concentrations. *B*, comparison of transient absorption spectra acquired using 130-fs excitation flashes at 850 nm in ultrafast studies of the primary photochemistry. RC concentrations and laser excitation conditions were matched. The spectra shown were acquired at 1 ns after the flash to minimize the contribution of shorter lived states. The relative yields of $P^+H_B^-$ (determined by the magnitude of bleaching of the band of H_B at 525–528 nm) agree well with those measured for the $P^+Q_B^-$ yields in the ms screening assay (*A*).

phytin substitutes for B_B. Whereas ET from P* to this new cofactor takes place in ~10 ps, ET onward to H_B does not occur (18), creating another, different, bottleneck in the quest for efficient use of the B side cofactors for transmembrane charge separation. Similar issues occur at the final step of ET from H_B to Q_B, which has a yield of only ~40% as mentioned above. The rate of this ET reaction is $\sim(4\ ns)^{-1}$, whereas the rate of competing charge recombination of $P^+H_B^-$ is $\sim(3\ ns)^{-1}$ (39). For comparison, the rates of the corresponding reactions on the A side are $(200\ ps)^{-1}$ and $\sim(20\ ns)^{-1}$.

To sample a larger number of variants and remove much of the prejudice inherent in rational design schemes, a directed molecular evolution approach has been adopted for engineering of the RC to enable efficient B branch ET. Directed molecular evolution has been applied to the discovery of new functions, increased expression, increased stability, and enhanced activity for many proteins (for review, see Refs. 52, 53) but has had relatively limited application to membrane proteins (*e.g.* Refs. 54–57). The present study merges principles of both rational design and directed molecular evolution to generate versions of the heterotrimeric, protein-cofactor RC complex that have acquired increased ability to utilize a vestigial ET pathway for transmembrane charge separation.

The mutagenesis employed here is best termed "semirandom" and relies on oligonucleotide cassettes rather than error-prone PCR or fragment shuffling. The rationale for this approach is based on knowledge of the structure, awareness of the substitutions that have been tried before, the concern that massively random mutagenesis will produce RCs with assembly and/or stability problems, the difficulties imposed by the high degree of sequence similarity between the *puf*L and *puf*M genes (especially in highly conserved regions that surround the cofactors), and the fact that their coding regions overlap (Fig. 2). Because this approach has worked well here for these genes embedded in the polycistronic *puf* operon, it is likely that the chosen mutagenesis strategy could be applied to many gene clusters encoding transmembrane complexes where components share a high degree of sequence similarity, a common occurrence in sequence data emerging from representatives of all kingdoms.

Directional cloning of cassettes required significant downsizing and engineering of the broad host range expression vector and was enabled by synthetic biology. Surprisingly, the yield of RCs expressed from the new, partially synthetic platform vector was 2-fold greater than the yield obtained from the original expression plasmid. This result may be due to differences in plasmid copy number and/or unexpected changes in (i) transcript stability, (ii) codon preferences, or (iii) modification of regulatory elements that occurred as a result of the engineering that was required.

In the initial round of saturation mutagenesis at the L181 site, surprises were encountered when yields of B side ET were found to be highest in RCs carrying His, Asn, Asp, and Gln mutations. Numerous RCs carrying single mutations at this site have been reported previously (9, 11, 58), but none of these studies had ever suggested that any of the above residues would match or exceed a Tyr at L181 in enhancing B branch activity or that the functional consequences of a Glu substitution would be similar to those conferred by a Tyr substitution (Fig. 4). In fact, considering that placement of an acidic residue close to B_A in the G(M201)D RC disfavors ET to the A side (12), it was surprising that an Asp substitution at L181 near B_B had the opposite effect, enabling more B branch activity. Similar effects observed for the polarizable His, Asn, Asp, and Gln residues at L181 cannot all be attributable to a common fundamental mechanism, but all of these substitutions will influence, rather unpredictably, the dielectric environment of the cofactors involved in the initial electron transfer reactions. The close parallel effects on B side ET for the Asn/Asp and Gln/Glu pairs, with the smaller Asn/Asp substitutions producing RCs with larger yields of B side ET, are noteworthy. In general, an assortment of uncharged substitutions at the L181 site is tolerated with neutral functional consequences; an additional surprise is that substitutions of both small (Gly, Ala) and large (Trp) residues produce nearly equivalent yields of $P^+Q_B^-$.

Although substitutions at the L216 site (regardless of whether they are accompanied by the Ala substitutions at L212–213) do not increase the amount of reduced quinone, trends are observed, some of which can be related to amino acid

properties. In general, large residues at the L216 site result in lower yields of reduced quinone. RCs in which ionizable residues are substituted at the L216 site, when in combination with the Ala substitutions at L212–213, either fail to assemble or perform poorly in the functional assay. It is possible that substitutions within this region of the Q_B binding site affect its occupancy. A disappointment is that the Trp substitution at this site does not result in increased ET from H_B to Q_B whereas the conserved Trp residue at the symmetry-related M250 site is critical for efficient ET from H_A to Q_A in the wild-type RC (33). These results suggest that targeting of residues based on their relationship to the C_2 symmetry axis in this region of the RC is less productive and emphasize that a more random, evolutionary approach will be required to enhance secondary electron transfer reactions of the B pathway.

Overall, the results reported herein validate the experimental strategy and underscore the plasticity of the RC in accommodating substitutions that result in a range of B branch activity. A subset of the new mutant RCs displays increased quinone reduction by the exclusive use of B branch cofactors. Unexpected, productive combinations of amino acid substitutions that previously have not been discovered by rational design were revealed by the approach described herein. Realization of these mutant RCs was enabled by miniaturization at two screening steps (expression testing and spectroscopic assays) and automation of protein purification and time-resolved spectroscopy. A system is now in place whereby mutant RCs with altered ET functionalities can be identified rapidly as candidates for more exhaustive functional characterization and iterative engineering to produce next generation RCs with desired ET capabilities, even those that are unimagined by Nature.

Acknowledgments—We thank Craig Luehr for optimization of scripts for automated protein purification and Elizabeth Landorf for assistance with adaptation of molecular biology methods to higher throughput on the liquid-handling robot.

REFERENCES

1. Allen, J. P., Feher, G., Yeates, T. O., Komiya, H., and Rees, D. C. (1987) Structure of the reaction center from *Rhodobacter sphaeroides* R-26: the cofactors. *Proc. Natl. Acad. Sci. U.S.A.* **84,** 5730–5734
2. Chang, C. H., el-Kabbani, O., Tiede, D., Norris, J., and Schiffer, M. (1991) Structure of the membrane-bound protein photosynthetic reaction center from *Rhodobacter sphaeroides*. *Biochemistry* **30,** 5352–5360
3. Deisenhofer, J., Epp, O., Miki, K., Huber, R., and Michel, H. (1985) Structure of the protein subunits in the photosynthetic reaction center from *Rhodopseudomonas viridis* at 3 Å resolution. *Nature* **318,** 618–624
4. Ermler, U., Fritzsch, G., Buchanan, S. K., and Michel, H. (1994) Structure of the photosynthetic reaction centre from *Rhodobacter sphaeroides* at 2.65 A resolution: cofactors and protein-cofactor interactions. *Structure* **2,** 925–936
5. Dashdorj, N., Xu, W., Cohen, R. O., Golbeck, J. H., and Savikhin, S. (2005) Asymmetric electron transfer in cyanobacterial photosystem I: charge separation and secondary electron transfer dynamics of mutations near the primary electron acceptor A0. *Biophys. J.* **88,** 1238–1249
6. Guergova-Kuras, M., Boudreaux, B., Joliot, A., Joliot, P., and Redding, K. (2001) Evidence for two active branches for electron transfer in photosystem I. *Proc. Natl. Acad. Sci. U.S.A.* **98,** 4437–4442
7. Joliot, P., and Joliot, A. (1999) *In vivo* analysis of the electron transfer within photosystem I: are the two phylloquinones involved? *Biochemistry* **38,** 11130–11136
8. Ramesh, V. M., Gibasiewicz, K., Lin, S., Bingham, S. E., and Webber, A. N. (2004) Bidirectional electron transfer in photosystem I: accumulation of A0- in A-side or B-side mutants of the axial ligand to chlorophyll A0. *Biochemistry* **43,** 1369–1375
9. Wakeham, M. C., and Jones, M. R. (2005) Rewiring photosynthesis: engineering wrong-way electron transfer in the purple bacterial reaction centre. *Biochem. Soc. Trans.* **33,** 851–857
10. Bylina, E. J., Kirmaier, C., McDowell, L., Holten, D., and Youvan, D. C. (1988) Influence of an amino-acid residue on the optical properties and electron transfer dynamics of a photosynthetic reaction centre complex. *Nature* **336,** 182–184
11. DiMagno, T. L., PD, Reddy, N. R., Small, G. J., Norris, J. R., Schiffer, M., and Hanson, D. K. (1998) Protein-chromophore interactions: spectral shifts report the consequences of mutations in the bacterial photosynthetic reaction center. *Spectrochim. Acta Part A* **54,** 1247–1267
12. Heller, B. A., Holten, D., and Kirmaier, C. (1996) Effects of Asp residues near the L-side pigments in bacterial reaction centers. *Biochemistry* **35,** 15418–15427
13. Katilius, E., Babendure, J. L., Katiliene, Z., Lin, S., Taguchi, A. K. W., and Woodbury, N. W. (2003) Manipulations of the B-side charge-separated states' energetics in the *Rhodobacter sphaeroides* reaction center. *J. Phys. Chem.* **107,** 12029–12034
14. Williams, J. C., Alden, R. G., Murchison, H. A., Peloquin, J. M., Woodbury, N. W., and Allen, J. P. (1992) Effects of mutations near the bacteriochlorophylls in reaction centers from *Rhodobacter sphaeroides*. *Biochemistry* **31,** 11029–11037
15. Allen, J. P., and Williams, J. C. (1995) Relationship between the oxidation potential of the bacteriochlorophyll dimer and electron transfer in photosynthetic reaction centers. *J. Bioenerg. Biomembr.* **27,** 275–283
16. de Boer, A. L., Neerken, S., de Wijn, R., Permentier, H. P., Gast, P., Vijgenboom, E., and Hoff, A. J. (2002) B-branch electron transfer in reaction centers of *Rhodobacter sphaeroides* assessed with site-directed mutagenesis. *Photosynth. Res.* **71,** 221–239
17. Heller, B. A., Holten, D., and Kirmaier, C. (1995) Control of electron transfer between the L- and M-sides of photosynthetic reaction centers. *Science* **269,** 940–945
18. Katilius, E., Turanchik, T., Lin, S., Taguchi, A. K. W., and Woodbury, N. W. (1999) B-side electron transfer in a *Rhodobacter sphaeroides* reaction center mutant in which the B-side monomer bacteriochlorophyll is replaced with bacteriopheophytin. *J. Phys. Chem. B* **103,** 7386–7389
19. Kirmaier, C., Gaul, D., DeBey, R., Holten, D., and Schenck, C. C. (1991) Charge separation in a reaction center incorporating bacteriochlorophyll for photoactive bacteriopheophytin. *Science* **251,** 922–927
20. Kirmaier, C., Laible, P. D., Czarnecki, K., Hata, A. N., Hanson, D. K., Bocian, D. F., and Holten, D. (2002) Comparison of M-side electron transfer in *R. sphaeroides* and *R. capsulatus* reaction centers. *J. Phys. Chem. B* **106,** 1799–1808
21. McDowell, L. M., Kirmaier, C., and Holten, D. (1990) Charge transfer and charge resonance states of the primary electron donor in wild-type and mutant bacterial reaction centers. *Biochim. Biophys. Acta* **1020,** 239–246
22. Watson, A. J., Fyfe, P. K., Frolov, D., Wakeham, M. C., Nabedryk, E., van Grondelle, R., Breton, J., and Jones, M. R. (2005) Replacement or exclusion of the B-branch bacteriopheophytin in the purple bacterial reaction centre: the H(B) cofactor is not required for assembly or core function of the *Rhodobacter sphaeroides* complex. *Biochim. Biophys. Acta* **1710,** 34–46
23. de Boer, A. L., Neerken, S., de Wijn, R., Permentier, H. P., Gast, P., Vijgenboom, E., and Hoff, A. J. (2002) High yield of B-branch electron transfer in a quadruple reaction center mutant of the photosynthetic bacterium *Rhodobacter sphaeroides*. *Biochemistry* **41,** 3081–3088
24. Laible, P. D., Kirmaier, C., Udawatte, C. S., Hofman, S. J., Holten, D., and Hanson, D. K. (2003) Quinone reduction via secondary B-branch electron transfer in mutant bacterial reaction centers. *Biochemistry* **42,** 1718–1730
25. Wakeham, M. C., Frolov, D., Fyfe, P. K., van Grondelle, R., and Jones, M. R. (2003) Acquisition of photosynthetic capacity by a reaction centre that lacks the Q_A ubiquinone: possible insights into the evolution of reaction centres? *Biochim. Biophys. Acta* **1607,** 53–63
26. Kirmaier, C., Holten, D., Bylina, E. J., and Youvan, D. C. (1988) Electron transfer in a genetically modified bacterial reaction center containing a

heterodimer. *Proc. Natl. Acad. Sci. U.S.A.* **85,** 7562–7566
27. Heller, B. A., Holten, D., and Kirmaier, C. (1995) Characterization of bacterial reaction centers having mutations of aromatic residues in the binding site of the bacteriopheophytin intermediary electron carrier. *Biochemistry* **34,** 5294–5302
28. Robles, S. J., Breton, J., and Youvan, D. C. (1990) Partial symmetrization of the photosynthetic reaction center. *Science* **248,** 1402–1405
29. Taguchi, A. K., Stocker, J. W., Alden, R. G., Causgrove, T. P., Peloquin, J. M., Boxer, S. G., and Woodbury, N. W. (1992) Biochemical characterization and electron-transfer reactions of sym1, a *Rhodobacter capsulatus* reaction center symmetry mutant which affects the initial electron donor. *Biochemistry* **31,** 10345–10355
30. Haffa, A. L., Lin, S., Lobrutto, R., Williams, J. C., Taguchi, A. K., Allen, J. P., and Woodbury, N. W. (2005) Environmental control of primary photochemistry in a mutant bacterial reaction center. *J. Phys. Chem. B* **109,** 19923–19928
31. Kirmaier, C., He, C., and Holten, D. (2001) Manipulating the direction of electron transfer in the bacterial reaction center by swapping Phe for Tyr near BChl(M) (L181) and Tyr for Phe near BChl(L) (M208). *Biochemistry* **40,** 12132–12139
32. Kirmaier, C., Weems, D., and Holten, D. (1999) M-side electron transfer in reaction center mutants with a lysine near the nonphotoactive bacteriochlorophyll. *Biochemistry* **38,** 11516–11530
33. Coleman, W. J., Bylina, E. J., Aumeier, W., Siegl, J., Eberl, U., Heckmann, R., Ogrodnik, A., Michel-Beyerle, M. E., and Youvan, D. C. (1990) in *Structure and Function of Bacterial Photosynthetic Reaction Centers* (Michel-Beyerle, M. E., ed) pp. 273–281, Springer-Verlag, New York
34. Coleman, W. J., and Youvan, D. C. (1993) Atavistic reaction centre. *Nature* **366,** 517–518
35. Kirmaier, C., Laible, P. D., Hanson, D. K., and Holten, D. (2003) B-side charge separation in bacterial photosynthetic reaction centers: nanosecond time scale electron transfer from H_B^- to Q_B. *Biochemistry* **42,** 2016–2024
36. Li, J., Coleman, W. J., Youvan, D. C., and Gunner, M. R. (2000) Characterization of a symmetrized mutant RC with 42 residues from the Q_A site replacing residues in the Q_B site. *Photosynth. Res.* **64,** 41–52
37. Paddock, M. L., Chang, C., Xu, Q., Abresch, E. C., Axelrod, H. L., Feher, G., and Okamura, M. Y. (2005) Quinone (Q_B) reduction by B-branch electron transfer in mutant bacterial reaction centers from *Rhodobacter sphaeroides*: quantum efficiency and x-ray structure. *Biochemistry* **44,** 6920–6928
38. Chuang, J. I., Boxer, S. G., Holten, D., and Kirmaier, C. (2006) High yield of M-side electron transfer in mutants of *Rhodobacter capsulatus* reaction centers lacking the L-side bacteriopheophytin. *Biochemistry* **45,** 3845–3851
39. Kee, H. L., Laible, P. D., Bautista, J. A., Hanson, D. K., Holten, D., and Kirmaier, C. (2006) Determination of the rate and yield of B-side quinone reduction in *Rhodobacter capsulatus* reaction centers. *Biochemistry* **45,** 7314–7322
40. Laible, P. D., Kirmaier, C. K., Holten, D., Tiede, D. M., Schiffer, M., and Hanson, D. K. (1998) in *Photosynthesis: Mechanisms and Effects* (Garab, G., ed) pp. 849–852, Kluwer, Dordrecht
41. Wakeham, M. C., Goodwin, M. G., McKibbin, C., and Jones, M. R. (2003) Photoaccumulation of the $P^+Q_B^-$ radical pair state in purple bacterial reaction centres that lack the Q_A ubiquinone. *FEBS Lett.* **540,** 234–240
42. Sambrook, J., Fritsch, E., and Maniatis, T. (1989) *Molecular Cloning: A Laboratory Manual*, 2nd Ed., Cold Spring Harbor Laboratory, Cold Spring Harbor, NY
43. Kovach, M. E., Elzer, P. H., Hill, D. S., Robertson, G. T., Farris, M. A., Roop, R. M., 2nd, and Peterson, K. M. (1995) Four new derivatives of the broad-host-range cloning vector pBBR1MCS, carrying different antibiotic-resistance cassettes. *Gene* **166,** 175–176
44. Bylina, E. J., Robles, S. J., and Youvan, D. C. (1988) Directed mutations affecting the putative bacteriochlorophyll-binding sites in the light-harvesting I antenna of *Rhodobacter capsulatus. Isr. J. Chem.* **28,** 73–78
45. Weaver, P. F., Wall, J. D., and Gest, H. (1975) Characterization of *Rhodopseudomonas capsulata*. *Arch. Microbiol.* **105,** 207–216
46. Kirmaier, C., Bautista, J. A., Laible, P. D., Hanson, D. K., and Holten, D. (2005) Probing the contribution of electronic coupling to the directionality of electron transfer in photosynthetic reaction centers. *J. Phys. Chem. B* **109,** 24160–24172
47. Bylina, E. J., Ismail, S., and Youvan, D. C. (1986) Plasmid pU29, a vehicle for mutagenesis of the photosynthetic *puf* operon in *Rhodopseudomonas capsulata*. *Plasmid* **16,** 175–181
48. Bylina, E. J., Jovine, R. V. M., and Youvan, D. C. (1989) A genetic system for rapidly assessing herbicides that compete for the quinone binding site of photosynthetic reaction centers. *Bio/Technology* **7,** 69–74
49. Youvan, D. C., Ismail, S., and Bylina, E. J. (1985) *Gene* **33,** 19–30
50. Kirmaier, C., Laible, P. D., Hindin, E., Hanson, D. K., and Holten, D. (2003) *Chem. Phys.* **294,** 305–318
51. Hanson, D. K., Baciou, L., Tiede, D. M., Nance, S. L., Schiffer, M., and Sebban, P. (1992) In bacterial reaction centers protons can diffuse to the secondary quinone by alternative pathways. *Biochim. Biophys. Acta* **1102,** 260–265
52. Yuan, L., Kurek, I., English, J., and Keenan, R. (2005) Laboratory-directed protein evolution. *Microbiol. Mol. Biol. Rev.* **69,** 373–392
53. Jäckel, C., Kast, P., and Hilvert, D. (2008) Protein design by directed evolution. *Annu. Rev. Biophys.* **37,** 153–173
54. Bokma, E., Koronakis, E., Lobedanz, S., Hughes, C., and Koronakis, V. (2006) Directed evolution of a bacterial efflux pump: adaptation of the *E. coli* TolC exit duct to the *Pseudomonas* MexAB translocase. *FEBS Lett.* **580,** 5339–5343
55. Dong, S., Rogan, S. C., and Roth, B. L. (2010) Directed molecular evolution of DREADDs: A generic approach to creating next-generation RASSLs. *Nat. Protocols* **5,** 561–573
56. Sarkar, C. A., Dodevski, I., Kenig, M., Dudli, S., Mohr, A., Hermans, E., and Plückthun, A. (2008) Directed evolution of a G protein-coupled receptor for expression, stability, and binding selectivity. *Proc. Natl. Acad. Sci. U.S.A.* **105,** 14808–14813
57. Wise, K. J., Gillespie, N. B., Stuart, J. A., Krebs, M. P., and Birge, R. R. (2002) Optimization of bacteriorhodopsin for bioelectronic devices. *Trends Biotechnol.* **20,** 387–394
58. Jia, Y., DiMagno, T. J., Chan, C. K., Wang, Z., Du, M., Hanson, D. K., Schiffer, M., Norris, J. R., Fleming, G. R., and Popov, M. S. (1993) Primary charge separation in mutant reaction centers of *Rhodobacter capsulatus. J. Phys. Chem.* **97,** 13180–13191